Data-driven Analysis of the Cost-Performance Trade-off of Reconfigurable Intelligent Surfaces in a Production Network

MARCO ROSSANESE, NEC Laboratories Europe GmbH, Germany
ANDRES GARCIA-SAAVEDRA, NEC Laboratories Europe GmbH, Spain
ANDRA ELENA LUTU, Telefonica Research, Spain
XAVIER COSTA PEREZ, NEC Laboratories Europe GmbH, Spain, and i2CAT Foundation, and ICREA

This paper presents a comprehensive study on the deployment of Reconfigurable Intelligent Surfaces (RIS) in urban environments with poor radio coverage. We focus on the city of London, a large metropolis where radio network planning presents unique challenges due to diverse geographical and structural features. Using crowd-sourced datasets, we analyze the Reference Signal Received Power (RSRP) from end-user devices to understand the existing radio coverage landscape of a major Mobile Network Operator (MNO). Our study identifies areas with poor coverage and proposes the deployment of RIS to enhance signal strength and coverage. We selected a set of potential sites for RIS deployment and, combining data from the MNO, data extracted from a real RIS prototype, and a ray-tracing tool, we analyzed the gains of this novel technology with respect to deploying more conventional technologies in terms of RSRP, coverage, and cost-efficiency.

To the best of our knowledge, this is the first data-driven analysis of the cost-efficiency of RIS technology in the production of urban networks. Our findings provide compelling evidence about the potential of RIS as a cost-efficient solution for enhancing radio coverage in complex urban mobile networks. More specifically, our results indicate that large-scale RIS technology, when applied in real-world urban mobile network scenarios, can achieve 72% of the coverage gains attainable by deploying additional cells with only 22% of their Total Cost of Ownership (TCO) over a 5-year timespan. Consequently, RIS technology offers around 3x higher cost-efficiency than other more conventional coverage-enhancing technologies.

CCS Concepts: • **Networks** → **Wireless access points, base stations and infrastructure**; **Network performance analysis**; **Mobile networks**.

Additional Key Words and Phrases: Reconfigurable Intelligent Surfaces, mobile network analysis, cost-efficiency

ACM Reference Format:
Marco Rossanese, Andres Garcia-Saavedra, Andra Elena Lutu, and Xavier Costa Perez. 2023. Data-driven Analysis of the Cost-Performance Trade-off of Reconfigurable Intelligent Surfaces in a Production Network. *Proc. ACM Netw.* 1, CoNEXT3, Article 12 (December 2023), 20 pages. https://doi.org/10.1145/3629134

1 INTRODUCTION

Reconfigurable Intelligent Surfaces (RIS) have recently emerged as a promising technology for next-generation mobile systems. These structures are known for their ability to reflect radio signals while altering some of their features, such as phase, which enables passive beamforming gains without the need for expensive and energy-consuming baseband processors or signal amplifiers.

Authors' addresses: Marco Rossanese, marco.rossanese@neclab.eu, NEC Laboratories Europe GmbH, Germany; Andres Garcia-Saavedra, andres.garcia.saavedra@neclab.eu, NEC Laboratories Europe GmbH, Spain; Andra Elena Lutu, andra.lutu@telefonica.com, Telefonica Research, Spain; Xavier Costa Perez, xavier.costa@neclab.eu, NEC Laboratories Europe GmbH, Spain and i2CAT Foundation, and ICREA.

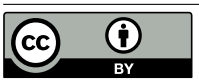

2834-5509/2023/12-ART12
https://doi.org/10.1145/3629134

Where RIS technology is really expected to outperform conventional Base Station (BS) technology (e.g., small cells, active relays, etc.) is in their energy efficiency. Their predominantly passive nature means they consume much less power, an aspect that is particularly valuable in outdoor environments, where maintaining power sources for base stations can be both logistically challenging and expensive. Another defining advantage of RIS is its minimal infrastructure needs, making it a cost-effective solution for outdoor mobile dead zones. This reduced demand for infrastructure, combined with their energy efficiency, underscores RIS's potential to reshape the future of mobile systems in a cost-effective way.

However, this technology is still in its nascent stage, with no RIS devices available in the market yet, and only a few prototypes discussed in the literature [28, 30, 37]. Hence, the cost-performance trade-off of this new technology in large-scale outdoor mobile network deployments remains an open question. To fill this gap, this paper investigates the integration of realistic RIS technology into a production mobile network in an outdoor urban environment.

We focus our study on a densely populated urban area within London that suffers poor radio coverage, which we empirically identify through performance measurements and user feedback reports from a commercial mobile network operator (MNO). Installing new radio equipment is an expensive process and one that must be carefully planned to optimally meet the capacity and coverage needs of the end users. Hence, we build a RIS model, which we developed from data collected from a real, cost-effective RIS prototype, and then we integrate such data-driven model into Wireless inSite [31] — a state-of-the-art 3D ray-tracing tool widely used in the research community for analyzing site-specific radio wave propagation and wireless communication systems [14, 17, 38]. This step is consistent with the approach that radio planning teams within commercial MNOs follow when planning to deploy new radio carriers and study "what-if" scenarios [7, 20]. With this, we examine the potential of large-scale RIS technology to improve coverage in these identified areas. We also conduct a comprehensive cost analysis, estimating the Capital Expenditure (CAPEX), the Operational Expenditure (OPEX), and the Total Cost of Ownership (TCO) associated with deploying RIS technology on a large scale. These costs are then compared with those related to using conventional BS technology, allowing us to evaluate the cost-efficiency of RIS technology in improving coverage in areas currently underserved by the incumbent MNO cells.

Existing literature has significantly enriched our understanding of RIS technology, offering valuable insights into optimal placement, configuration, and theoretical models [4, 15, 16, 18, 26, 29]. However, these studies predominantly focus on indoor or small scenarios and are based on idealized models. A brief review of this and other related literature can be found in §6. *Our paper is, to the best of our knowledge, the first data-driven study to delve into the practical implications of deploying real-world RIS technology in production mobile networks,* thereby offering a novel perspective on the potential of RIS in shaping next-generation mobile systems. Our findings suggest that, in a real urban context, large-scale RIS can achieve 72% of the coverage gains that additional MNO cells may obtain. Remarkably, this is accomplished with just 22% of the TCO over a five-year period. As a result, *our work finds compelling evidence that RIS may provide ∼3x higher cost-efficiency than conventional technologies that require costly infrastructure and energy-consuming electronics.*

The structure of this paper is as follows. §2 provides background information on RIS, introduces a real RIS prototype, and conducts a cost analysis. §3 utilizes datasets to identify coverage issues in real urban scenarios, validates a ray tracing tool for analysis, and presents deployment options for large-scale RIS structures. Subsequently, §4 compares the cost-efficiency of RIS technology in providing coverage gains in these scenarios with other, more expensive but high-performing, alternatives. §6 reviews the related literature, and §7 concludes the paper.

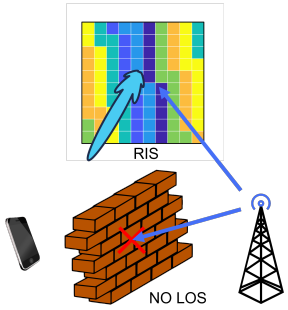

Fig. 1. Common RIS use case.

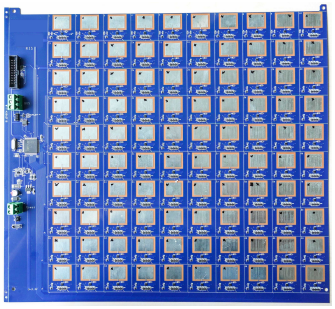

Fig. 2. RIS prototype (from [32]).

2 RECONFIGURABLE INTELLIGENT SURFACES

In this section, we first provide a brief introduction to Reconfigurable Intelligent Surfaces (§2.1); we then introduce a real prototype and build a data-driven model (§2.2); and we conclude the section with a comparative cost analysis of RIS technology and more conventional BS technologies (§2.3).

2.1 A Primer on Reconfigurable Intelligent Surfaces

Reconfigurable Intelligent Surfaces (RIS) are engineered structures that can modify the way radio waves behave when they hit the surface. By changing its configuration, an RIS can control the direction, strength, polarization, and other properties of the reflected radio waves. RIS is designed to be as passive as possible in terms of power consumption; in fact, no RF chains are involved, as well as no amplification or digital signal processors. In the literature, this kind of RIS is commonly defined as "passive" because the signal is neither amplified nor regenerated before retransmission, although it involves a small amount of power for functioning; on the other hand, an active RIS can improve the signal before retransmission on the cost of high power consumptions [39].

RIS can be implemented using a variety of different types of surfaces, which can span from very sophisticated metasurfaces to arrays of antennas used as reflectors. A metasurface is made of metamaterials, a type of material that has been engineered to have properties that are not found in naturally occurring materials. They are typically composed of arrays of small metallic or dielectric elements whose behavior can be externally controlled. They are complex to build but can unlock many various features [23]. The alternative is to utilize an array of passive reflecting elements, such as small metallic patches or dielectric rods, to reflect impinging radio waves in a specific direction. Such property is usually achieved by adapting conventional beamforming techniques where the individual reflecting elements apply (different) phase shifts to the reflected signals passively. In this way, the multiple reflections can interfere constructively in the desired direction, while they cancel each other out in other directions [11].

RIS technology enables smart environments [10] where the wireless channel is yet another knob subject of optimization. This contrasts with the conventional view of treating the channel as a given (or estimated) parameter. Smart environments will be crucial for the next-generation mobile systems, and can improve the reliability of communication systems by increasing path diversity between BSs and user devices (UE), as depicted in Fig. 1. An example of a specific RIS application is improving the coverage of cellular networks in hard-to-reach areas like underground tunnels or inside buildings. Another example is using RIS in radar systems to improve the accuracy and resolution of location information. Lastly, from a security perspective, using RIS to focus radio waves toward specific indoor locations can enhance the security of private networks. By adjusting the signal strength to be stronger in the desired locations and weaker in non-essential areas, it

can be more difficult for malicious individuals to gain unauthorized access to the network by intercepting the signals in unwanted areas [5]. We will focus on the former use case in this paper: coverage assistance in complex urban scenarios.

2.2 Empirical Modeling of a Reconfigurable Intelligent Surface Prototype

Despite the prospects mentioned above, RIS is not a mature technology; commercial off-the-shelf solutions are lagging and only a few prototypes have been implemented by researchers in the RIS community. In the following, we build a realistic model of RIS technology that we can use in our analysis at scale. To this end, we use the dataset provided by [32] with measurements of an inexpensive RIS prototype.[1] We next briefly summarize the RIS design and the measurements provided in the dataset. The interested reader can find more details in [32].

The RIS system consists of multiple boards, each of which provides a 10x10 array of patch antenna elements. Each antenna element operates in sub-6GHz carrier frequency with a bandwidth of 100 MHz and reflects impinging signals with a phase shift controlled by a 3-bit RF switch. Every RF switch is in turn configured by a microcontroller unit (MCU) that, supported by a grid of buses, can access every RF switch in the board to set the desired phase shift on each antenna element. The reconfiguration time of the RIS board is approximately 35 ms and its consumption (mostly due to the MCU) is 60 mW. Fig. 2 depicts a photograph of the prototype.

A dataset with measurements collected in an anechoic chamber is provided by [32]. An anechoic chamber is a controlled environment isolated from external electromagnetic interference and with minimal internal reflections. Therefore, the channel between the transmitter and the receiver only consists of a direct line-of-sight (LoS) link. It is important to note that maintaining an LoS channel is crucial for this purpose as, otherwise, it may be challenging to distinguish between the contribution reflected by the RIS and other multipath scattered signal components.

To collect this data, a RIS board was placed at one extreme of the room, on a rotating table attached to an antenna (TX) that transmits OFDM-modulated signals, as shown in Fig. 3. This setup allows setting the angle of arrival (AoA) of the LoS link between TX and RIS and between RIS and a receiving antenna (RX), which is placed in the other extreme of the room and demodulates those signals. The TX and RX are implemented using two horn antennas that operate within a frequency range of 1-8 GHz and show a gain of 13.5 dBi, as well as a voltage standing wave ratio (VSWR) of approximately 1 at the operating frequency of the RIS. The TX is positioned at a distance of 1.1 m from the first top-left element of the RIS, with a fixed azimuth and elevation angles of 90° and -33°, respectively. In turn, the RX is located in front of the RIS with an azimuth angle of 90° and an elevation angle of 3°, positioned 6.3 m away from the top-left antenna element. The rotating table and the RIS configuration are controlled by an off-the-shelf computer outside the room.

The signal sent to the TX is generated by a dual-channel transceiver, specifically the USRP model B210, which can provide continuous RF coverage between 70 MHz and 6 GHz. On the RX side, another USRP B210 is used to sample and decode the incoming signals. Both USRPs utilize the srsRAN software, an open-source SDR 4G/5G suite from Software Radio Systems (SRS), capable of processing 3GPP-compliant OFDM signals. The TX-side USRP is specifically employed to generate a continuous stream of OFDM QPSK-modulated symbols with a bandwidth of 5 MHz, transmission power of -30 dBm per subcarrier, and numerology that meets the requirements of 3GPP specifications. Meanwhile, the RX-side USRP measures the received power of the reference signal (RSRP), averaged across the signal bandwidth.

The dataset includes measurements with a pre-defined codebook of RIS configurations. Each configuration is designed to orient the primary beam of the RIS reflection pattern toward a specific

[1]The dataset is publicly available in https://github.com/marcantonio14/RIS-Power-Measurements-Dataset.

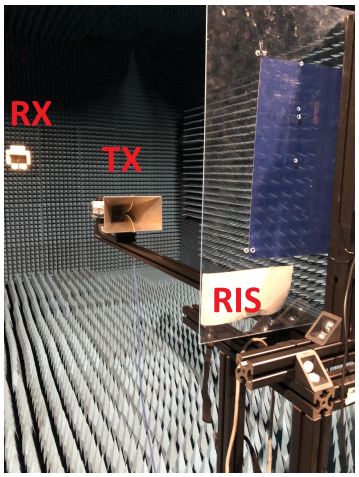

Fig. 3. Experimental setup (from [32]).

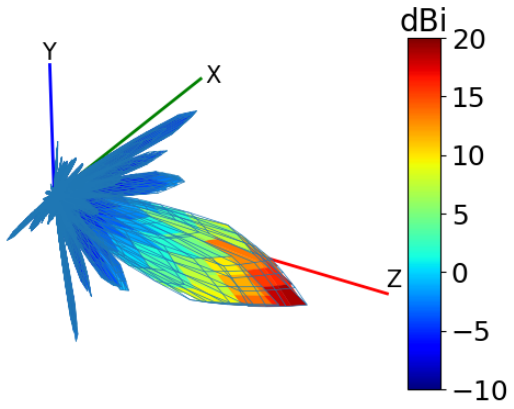

Fig. 4. 3D RIS radiation pattern.

and unique direction in space. Specifically, the main beam is scanned within the azimuthal range of $[-90°, 90°]$ and the elevation range of $[-45°, 45°]$, with a step size of 3° in both cases. As a result, the codebook consists of a total of 1891 distinct configurations. The turntable is set to move within the azimuthal range of $[-90°, 90°]$ with a step size of 3°. The angle between the surface of the RIS and the RX is denoted as θ_r. For each θ_r value, which corresponds to an equal rotation angle of the table, the RIS board iterates through all the configurations in the codebook, and RSRP power samples are collected. In total, the dataset contains 6.5M samples.

As the channel within the anechoic chamber remains quasi-static, we conclude that the primary source of noise affecting the RSRP measurements in the dataset stems from imperfections in either the electronic components utilized in the RIS or the constituent parts of the chamber. To enhance the quality of the data, we employed a Savitzky–Golay filter, a widely used method for smoothing data and performing calculations based on noisy input data. Nevertheless, such imperfections are inherent in inexpensive RIS technologies and are usually ignored in the RIS literature, which relies upon idealized RIS models. Hence, building a data-driven 3D reflection model is key to making a realistic analysis of the impact of real-world RIS in production mobile networks, which is our goal.

To this end, using the available data from that measurement campaign, we first re-create 2D reflection patterns for all different RIS configurations in the dataset. In order to recreate 3D reflection patterns, it is crucial to have data from two 2D planes that are orthogonal to each other. In our specific case, as the relative difference in elevation between the TX, RIS, and RX is constant, we can only rely on the azimuth plane (with a fixed elevation). Nevertheless, due to the squared geometry of the prototype, we can take advantage of the symmetry between the azimuth and elevation planes in the reflection patterns for interpolation. As a result, we are able to construct 3D reflection patterns for all the configurations in the RIS prototype, as exemplified in Fig. 4. *This information is essential to assess realistic (imperfect) RIS technologies at scale, as we will present later.*

2.3 Cost Analysis

Finally, we delve into the costs associated with implementing RIS technology for coverage support in outdoor scenarios, compared to the deployment of additional BS technologies. This analysis considers two RIS scales with 40x40 and 80x80 antenna elements, respectively. Note that, at sub-6GHz, these are large-scale structures of 8.18 m^2 and 32.72 m^2, respectively.

The costs that an MNO must bear can be categorized into capital expenditures (CAPEX) and operating expenditures (OPEX). CAPEX encompasses the one-time costs required to deploy a solution, including acquiring and putting the assets into operation. Conversely, OPEX aggregates the costs associated with running the solution, such as maintenance, electricity, cooling, etc.

When it comes to solutions for coverage support, CAPEX can be broken down into equipment (antennas, baseband processors, etc.), the cost of the tower where the solution will be mounted, if needed, in compliance with the safety regulations of the country (with the EU as a reference), installation costs such as manpower to execute the deployment, and connection costs associated with fiber links for backhauling when required. As for OPEX, these expenses can be divided into rent (leasing of the space where the solution is deployed), operation and management (O&M), connection costs incurred by operating the backhaul network if required, and electricity costs incurred by baseband processors and signal amplifiers. To provide a clearer picture, we compare the costs associated with RIS deployments with the cost of conventional BS technologies: pico-cells, micro-cells, and common massive active antennas with 128 antenna elements. Table 1 dissects these costs, where OPEX are assumed per one year. Given the complexity of the task and the lack of data in the literature regarding cost models for BSs, we decided to include the values for CAPEX and OPEX from the very few available sources. The numbers in bold are the values we label as most reliable; the other values in the same table cell may be related to documents old in time and/or related to previous generations, e.g. 3G, but that could be of interest to the reader. Also, our internal connections inside the MNO helped us to determine the reliability of the costs from the different sources. For the RIS, instead, only one cost model is present in the literature [32], therefore the bold numbers refer to that, but we include also our new estimation based on our recent experience. Fig. 5 shows the Total Cost of Ownership (TCO), which sums CAPEX and OPEX for a timespan that ranges between one and five years.

In terms of CAPEX, for BS technologies, the connection costs play a significant role, with an average estimate of €33K as suggested in [33], followed by the tower costs with €20K (for micro and massive antenna cells), the installation costs with €10K (15K as stated in [21, 27]), and the equipment costs with €5K as reported in [24] (3K, 12K, and 20K as respectively declared in [21, 27, 33]). Hence, we also compare the costs of a micro-cell with integrated access and backhaul support (IAB), which uses wireless backhaul to mitigate some of these costs, especially connection costs. In contrast to these solutions, RIS is lightweight and easy to mount almost anywhere, therefore a tower is not really necessary — standard surfaces like billboards or walls suffice — and a simple control channel is required for configuration, inducing minimal connection costs [33]. Based on the cost analysis presented in [32] for the same RIS technology that we employ in this paper, the equipment costs are estimated at €12.8K for a large-scale 80x80 structure, and roughly 25% of that for a 40x40 structure. Based on our recent experience, we believe that the price for electronics proposed in [32] can be easily reduced to €1.2, yielding a total price for a unit cell of €1.35, and final prices of €2.1K and €8.5K for a 40x40 RIS and a 80x80 RIS, respectively. It is worth noting that these RIS costs are overly conservative, based on prices for electronic components available at conventional retailers. Mass RIS production may reduce these numbers substantially.

Concerning OPEX, conversely, the main contributor is energy consumption, which can reach peak power values spanning between 6 KW and 9 KW for micro and massive BS technology [9]. Given the conservative approach adopted in our analysis, we used the lower bound, 6KW, for the TCO estimation. Note that, though a massive-cell has a much larger number of antenna elements, the overall transmission power, which is distributed among all the available antenna elements, may be the same (and it is the same in our analysis later). Considering the electricity price in the Euro area in 2019 (pre-covid era), around 0.12 €/KWh [13], such consumption translates into €6.3K-€9.5K yearly. In comparison, the electricity bill of a pico-cell is negligible [6]. Rental costs are estimated

	40x40 RIS (k€)	80x80 RIS (k€)	Pico (k€)	Micro (k€)	Micro (IAB) (k€)	Massive (k€)
Equipment	**3.2**, 2.1	**12.8**, 8.5	**2**, 5[21]	**5**, 3[27] 12[33] 20[21]	**3**	**5.2**
Tower	**0**	**0**	**3**	**20**	**20**	**20**
Installation	**1.5**	**2**	**2**, 3 [21]	**10**, 15[21, 27]	**5**	**10**
Connection	**3**	**3**	**33**	**33**	**0**	**33**
Rent	**0.5**	**1**	**0.5**	**2.5**	**2.5**	**2.5**
O&M	**1**	**1**	**1**	**1**	**1**	**1**
Connection	**0**	**0**	**1**, 5[21]	**1**, 5[21]	**0**	**1**
Consumption	**0**	**0**	**0.1**	**6.3-9.5**	**3.1**	**6.3**

Table 1. CAPEX and OPEX for deploying a unit of conventional BS technology and RIS.

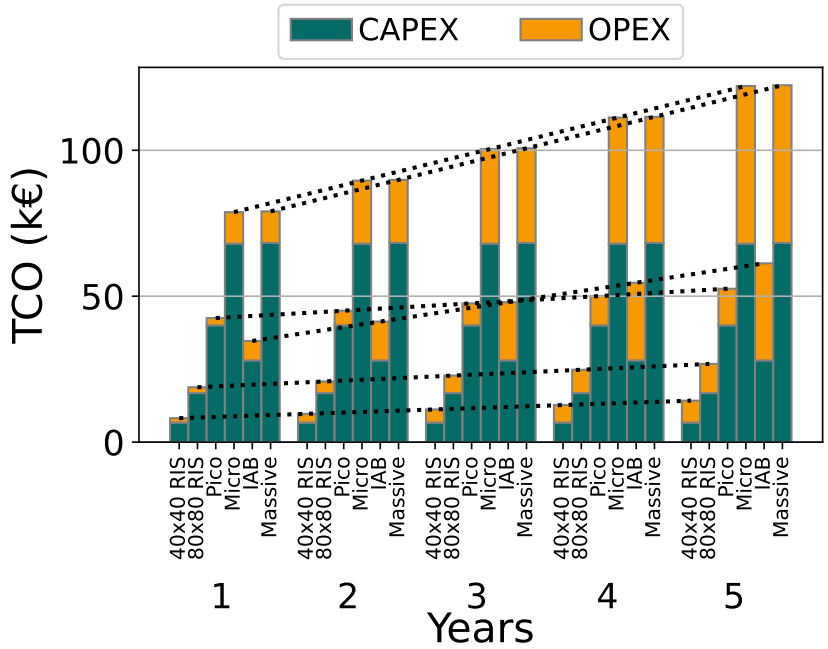

Fig. 5. TCO for a range of timespans for deploying a unit of conventional BS technology and RIS.

at around €2.5K, as stated in [24], O&M expenditures are estimated at around €1K as reported in [24], and backhauling of 1k as stated in [33] (5k for both Pico and Micro in [21]). Like with CAPEX, IAB can save 100% of the connection costs and around 50% of the electricity costs (the part associated with backhauling). For RIS, the energy consumption is very small, around 60 mW [32], and the control channel is extremely simple, which translates into a negligible electricity bill and connection costs. To estimate the costs associated with renting space to deploy large-scale RIS structures, we used market values for renting billboards [3]. Finally, we expect that RIS O&M costs should be considerably less than those for a micro-cell. However, in the absence of concrete data, we adopt a conservative approach and consider these costs to be on par.

When we aggregate the CAPEX and OPEX over a five-year period, an 80x80 RIS can potentially result in a TCO that is 78% lower than a micro- or massive-antenna cell (56% if IAB is supported) and 57% lower than a pico-cell. A 40x40 RIS further increases those savings by 88.5% and 77%, respectively. *These substantial cost-savings render RIS technology especially attractive for large-scale*

coverage extension. In the subsequent sections of this paper, we will delve into the performance of RIS in extending wireless coverage use cases and compare its cost-efficiency with other alternatives.

3 DATASETS, TOOLS, AND RIS DEPLOYMENTS

In this section, we first discuss the radio network topology of a major MNO in the UK. We then show that by analyzing radio coverage measurements collected from end-user devices connecting to this MNO, we can identify coverage gaps in its radio network, which impact the service of end-users. To address these gaps, we subsequently validate the effectiveness of a state-of-the-art ray-tracing tool, which enables us to evaluate the deployment of RIS in a representative target area to enhance the overall performance and coverage of the network.

3.1 Datasets

For our study, we rely on real-world datasets that we collect from a large commercial mobile network operating in the UK, with a major market share. We detail these datasets next.

Radio Network Topology. For our case study on the integration of RIS in outdoor mobile networks, we consider the topology of a production radio network, owned by a commercial mobile network in the UK. To keep up with the ever-increasing traffic demand, and to meet the end-user service expectations, the main approach operators choose today is the deployment of new radio channels to enhance their coverage within specific areas (e.g., hot spots where traffic demand is soaring). Enhancing radio coverage usually means that the operators install expensive physical hardware in strategic locations, which then they optimally configure in order to integrate within their respective radio access networks.

Our topology dataset captures the geographical location of all the radio cell sites the operator uses, the different radio sectors (i.e., carriers) deployed at each site, and their respective configuration. We confirm that the operator's main goal in terms of radio deployments is maximizing population coverage, thus prioritizing their deployments in areas with the highest population density (see Fig. 6a). This strategy is more obvious in the case of the ongoing 5G roll-out, where early deployment focused first on densely populated major metropolitan areas.

For the remainder of this paper, we focus on the mobile radio deployment the operator owns in London. Radio network planning within this type of large metropolis is a non-trivial task, since different geographical areas present different signal propagation patterns, bringing the challenge of tailoring the deployment to the location characteristics. Additionally, network engineers must account for user mobility, interference, load balancing, handovers, outage, and congestion management — all translating into configurations that are not easily updated afterward.

Radio Coverage Measurements. In an effort to continuously improve the quality of service, the operator monitors the radio coverage from the end-user perspective through crowd-sourced objective measurements combined with periodic surveys from the customer base, to capture their subjective experience. According to insights from periodic surveys shared by the operator, the radio coverage (or lack thereof) is often invoked as a root cause by subscribers who report low quality of experience. For our study, we focus on two commercial crowd-sourced datasets that the operator provided. Substantiating these with quality of experience measurements falls beyond the scope of this work. The two datasets are similar in that they capture radio signal strength metrics from the end-user device via code embedded in popular apps that run on the end-user equipment. In particular, we focus our analysis on the Reference Signal Received Power (RSRP). This is a metric that represents the average of reference signal power across a specified bandwidth (in the number of Resource Elements). It is a critical parameter that a User Equipment (UE) needs to measure for tasks such as cell selection, reselection, and handover in cellular communication systems.

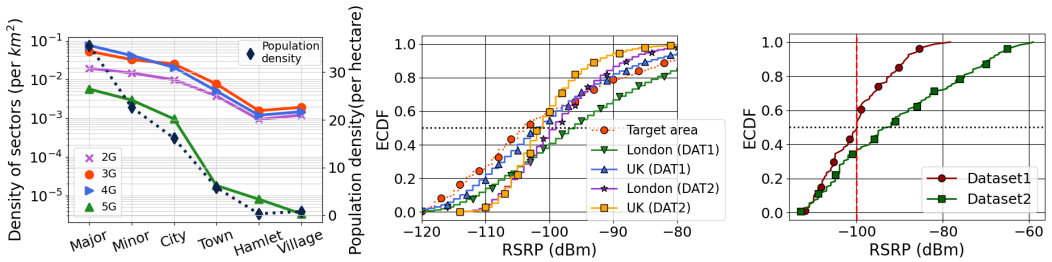

(a) Network Deployment. (b) Network coverage. (c) Target area coverage.

Fig. 6. We explore (a) the network deployment strategy of maximizing population coverage: the deployment density of radio sectors (i.e., radio antennas, per technology generation) the operator installs in different types of geographical areas (i.e., major/minor urban area, city, rural town, etc.) correlates with the median population density per area type, as published by the Office of National Statistics in the UK. We also show (b) the ECDF of the RSRP measurements we collect over different geographical areas (London, UK), in both Dataset1 (DAT1) and Dataset2 (DAT2). Finally, we focus on (c) the coverage within a specific target area, where we corroborate the measurements from both datasets we consider.

Dataset1 includes the median RSRP per tile unit over a 100x100m grid covering the areas of interest (namely, London, all UK). The median RSRP value per tile is derived from all the measurements captured within each tile over the same before-mentioned period of November 2022.

Dataset2 includes individual measurement samples of the RSRP metric from end-user devices collected during November 2022. The dataset includes more than 600,000 samples, each tagged with geographical coordinates and the corresponding radio sector identity.

These two datasets allow us to capture the coverage the operator provides over the entire country, and further zoom in on London (see Fig. 6b). In both datasets, we capture the wide variation of the RSRP across different geographies. We focus our analysis on London, which represents the main hub of innovation for the operator due to the high population density and increasing service demand. For ease of presentation, in the rest of this paper, we only focus on a specific target area within the city of London, which we select to demonstrate the impact of deploying RIS for coverage improvement of the production network. Nevertheless, our datasets and reach allow us to run a similar study in virtually any other area within the UK.

Ethical considerations. The data collection and retention at network middle-boxes and elements are in accordance with the terms and conditions of the MNO and the local regulations. All datasets we use in this work are covered by NDAs prohibiting any re-sharing with 3rd parties even for research purposes. Further, raw data has been reviewed and validated by the operator with respect to GPDR compliance (e.g., no identifier can be associated with a person), and data processing only extracts aggregated user information at the postcode level. No personal and/or contract information was available for this study, and none of the authors of this paper participated in the extraction and/or encryption of the raw data.

3.2 Target area for RIS deployment study

We based our decisions to determine suitable areas with poor radio coverage in the city of London on several factors, including the vicinity to mobile cells, which is a requirement for RIS operation [22], and the two datasets containing analytics on users' device feedback provided by the telco operator. We filtered the two datasets for RSRP below -100 dBm, which we define as bad coverage. This threshold is strongly dependent on the type of area, and it is usually determined with drive tests [36]. Since we are working in a residential area, we choose the value -100 dBm as RSRP threshold

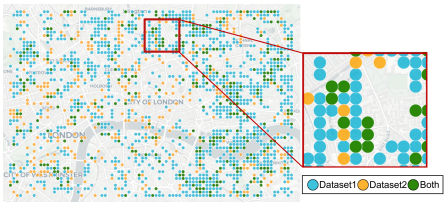

Fig. 7. Radio coverage map for the city of London with RSRP < -100 dBm.

Fig. 8. 3D model of a London area, location of cell sites, and potential RIS sites.

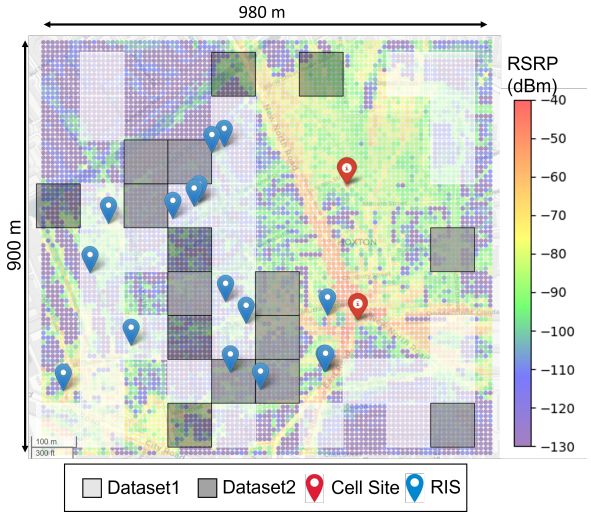

Fig. 9. Baseline RSRP with ray-tracing tool and with empirical datasets, location of cell sites, and potential RIS sites.

below which end-users experience service degradation and issue complaints to the operator. Fig. 7 summarizes the coverage of the datasets for November 2022.

From the identified set of areas with poor coverage, we selected an area of 980m x 900m depicted in Fig. 7 for further study in this paper. Nonetheless, our analysis can be extended to all other areas we have pinpointed. We divide the space into a grid, where each sector, or tile, is a square of 0.01 km^2 area. If we analyze the datasets specifically for this selected region, it becomes clear by looking at the CDF for RSRP in Fig. 6c that this area suffers from poor coverage for the 52% and 37% of the cases for Dataset1 and Dataset2, respectively.

3.3 Validation of ray-tracing tool

Fig. 8 illustrates a 3D model of the neighborhood we selected for this study, which we constructed from OpenStreetMap data. The model highlights the locations of two cell sites (CS1 and CS2) from the MNO under analysis. CS1 features six cells at a height of 15.5 meters, while CS2 comprises three cells at a height of 20 meters. Each cell is equipped with a 4G 60°-sectorial antenna operating in Band 1 with a transmission power of 40 dBm. The figure also proposes potential locations for the implementation of RIS technology, which we discuss later in more detail.

As mentioned above, we employ a ray-tracing tool called Wireless InSite [31] to evaluate the coverage enhancements achieved by RIS technology in this area. Therefore, an essential initial step is to verify the effectiveness of the tool for our analysis. To this end, in Fig. 9 we examine the coverage results that are provided by the nine cells using the ray-tracing tool and we compare these simulated results with the empirical data from the aforementioned datasets, which we depict in grey and white squares in the figure. The ray tracer provides mean RSRP samples at a granularity of 100 m^2, which we depict as colored circles in Fig. 9. To validate the tool, we compare the RSRP samples from the ray tracer with the overlapping empirical samples from the datasets. Fig. 10 shows a median error of 2.1 and 4.8 dB, with respect to Dataset1 and Dataset2, respectively, which we deem sufficiently small to rely on the ray-tracing solution for our analysis.

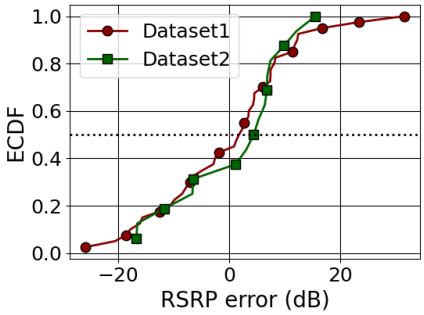

Fig. 10. ECDF of the error between the empirical RSRP samples in our datasets and the samples provided by a ray-tracing tool.

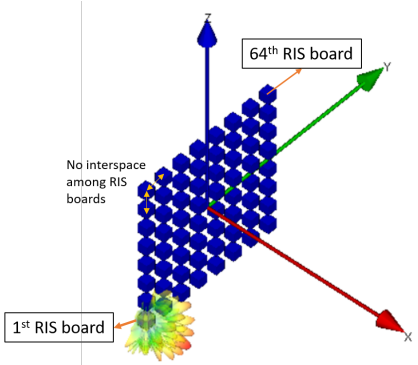

Fig. 11. Multiple RIS boards stacked together to form a larger RIS structure.

Table 2. Distance between potential RIS sites and MNO cell sites.

Site	A	B	C	D	E	F	G	H	I	J	K	L	M	N	O	P
CS1 (m)	411	411	484	763	368	586	590	290	300	278	525	336	324	386	375	481
CS2 (m)	136	135	262	659	291	497	591	66	480	472	580	432	428	457	244	300

3.4 RIS deployments

Once validated, the next step is to integrate a RIS model into the ray-tracing tool. Given the relatively recent emergence of RIS technology, it is challenging to capture inherent deficiencies, such as unexpected side lobes, from inexpensive electronics. Therefore, instead of simulating an ideal reflective surface, we use the realistic data-driven RIS model of an actual RIS prototype that we introduced in §2.2. To this end, we replicated an object with the same 3D reflection patterns that we derived in §2.2 (see Fig. 4). By employing such an experimentally-driven model, we can conduct a more realistic analysis using ray-tracing.

The RIS board evaluated in §2 comprises a 10x10 array of inexpensive antenna elements. However, such a small surface is insufficient to provide beamforming gains at the scale of the area we are examining [11]. Fortunately, the chosen RIS prototype supports the stacking of multiple boards to create larger structures [32], enabling us to model larger-scale RIS structures in our ray-tracing tool, as depicted in Fig. 11. In our analysis, we select squared arrays of RIS boards with varying sizes, which allows us to build RIS structures ranging from 20x20 antennas to 80x80 antennas. This approach allows us to assess the dimensions and costs required to deploy this technology in real outdoor environments.

The remaining question is to find suitable locations to deploy RIS technology. Three requirements must be met: (*i*) there must be good line-of-sight wireless links between an incumbent cell and the RIS structure, (*ii*) the power that may be harvested by a RIS is high enough to produce meaningful beamforming gains (note that a purely passive RIS is unable to amplify signals), and (*iii*) it should be close to poor coverage areas in order to be helpful. Given the highly heterogeneous nature of the urban environments under analysis, devising a systematic placement procedure is inherently challenging. Consequently, we identified potential RIS sites by locating relatively tall buildings near areas with poor coverage, which would help meet the requirements mentioned earlier.

As evident from Fig. 9, the incumbent MNO cell sites (represented as red pins on the map) primarily target the main streets and the eastern side of the neighborhood. This area includes a large park and a block of widely spaced houses. The open space is ideal for radio communication, a fact corroborated by the two datasets. However, coverage issues become apparent on the western side, where most areas experience an RSRP lower than -100 dBm, as indicated by both our datasets

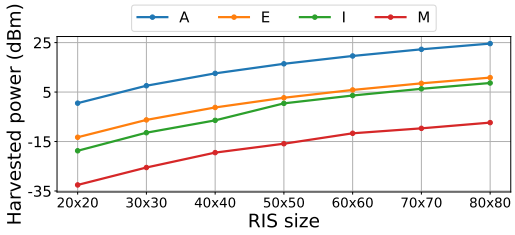

Fig. 12. Power harvested by RIS structures of different scales and at different locations.

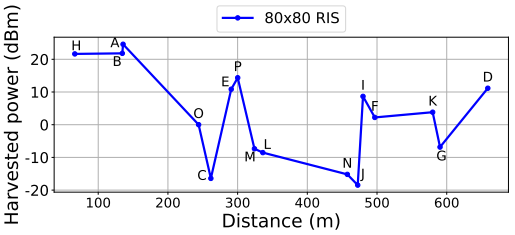

Fig. 13. Power harvested by 80x80 RIS as a function of their distance from the closest MNO cell.

and the ray-tracing tool. Therefore, we focus on our potential RIS deployments in this part of the neighborhood. This area comprises a cluster of low-rise houses surrounded by just a few buildings that are 30 meters or taller. We select 16 locations for potential RIS deployment that meet the aforementioned requirements, as shown in Figs. 8 and 9. These deployment sites are compatible with the sites the MNO would rent to deploy their own equipment. Table 2 presents the distance between each potential RIS site and the two MNO cell sites. The closest RIS deployment is 66 meters from a cell site, and the furthest is 659 meters away. To the best of our knowledge, at the time of writing, no other work in the literature assessed realistic RIS deployments at this scale.

For each potential RIS site, we deploy a RIS structure of varying sizes, and study the amount of power it can harvest for reflection. Fig. 12 displays these values for four different potential sites (A, E, I, M). The first observation is that power exhibits a logarithmic behavior with the size of the RIS, a phenomenon well-documented in the literature [34]. The second observation is that the environment plays a crucial role. For instance, sites I and M, which are at similar distances from a CS, experience significantly different power levels. To gain further insights, we show in Fig. 13 the amount of power that may be harvested (for reflection) by the largest RIS structure as a function of the distance to the closest CS. Sites A, B, and H, which receive substantial power from the southernmost CS, can harvest 20 dBm of power. However, site D, despite being over 600 meters away from the closest CS, can leverage its elevated height (38 meters) to harvest 11 dBm, which is more than the same RIS at site C, only 260 meters away from the closest MNO cell. Some other locations, such as C, M, and J, do not have a clear line-of-sight with an MNO cell, and the power they receive is mainly due to secondary paths, explaining the limited amount of power they can harvest. This irregular pattern underscores the difficulty of implementing a systematic methodology for deploying RIS in urban scenarios.

4 COST-PERFORMANCE TRADE-OFFS ANALYSIS

We next analyze the potential of RIS technology to enhance wireless coverage in a cost-efficient way. To avoid clutter in our presentation, in this section, we concentrate on eight potential RIS sites, namely C, M, F, I, E, P, H, and A. We selected these sites and ranked them in ascending order based on the power they receive from the best CS, as illustrated in Fig. 13.

We evaluate the network performance gains when deploying at these sites the large-scale RIS boards we previously analyzed in §2.3: a 40x40 RIS and an 80x80 RIS. To provide a comparative perspective, we also evaluate the RSRP, coverage, and cost-effectiveness improvements when deploying three different BS technologies at the same sites instead of RIS technology:

- Pico: An inexpensive pico-cell, with 20 dBm transmission power.
- Micro: An active antenna transmitting at 40 dBm, identical to the antennas of the micro-cells incumbent in the mobile network.
- Massive: An active array of 128 antenna elements transmitting at 40 dBm.

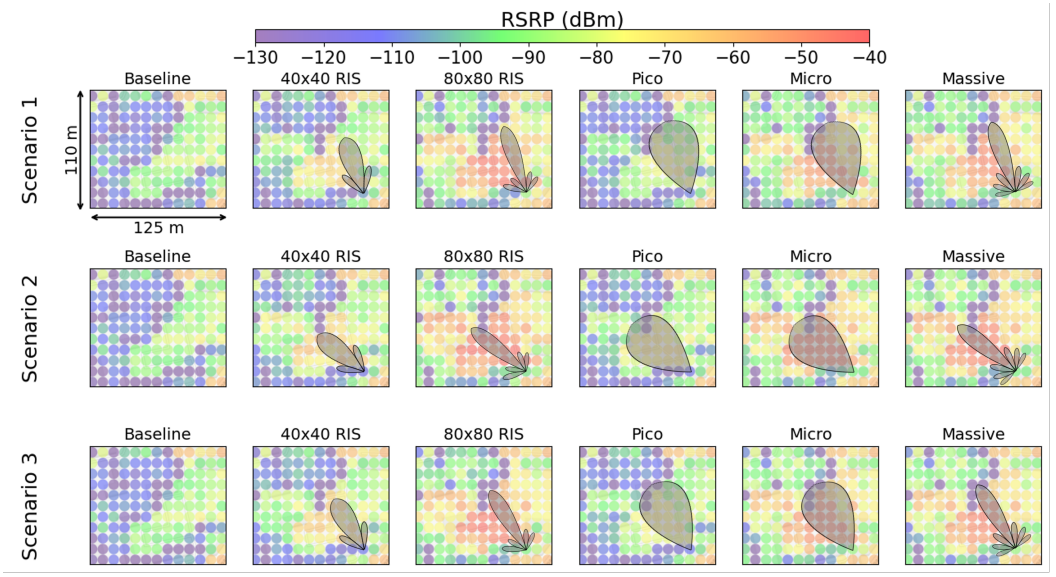

Fig. 14. RSRP in different *scenarios* (horizontal subplots) and solutions (vertical subplots) in RIS site A.

4.1 RSRP gains

We begin our analysis by investigating the power boost that each of the five previously mentioned solutions can provide at the selected sites. For each potential RIS site, we formulate a "scenario" by selecting a point experiencing poor RSRP in the vicinity, and then adjust the selected solution to optimize power at that location. For example, Fig. 14 presents three distinct scenarios for RIS site A (depicted in horizontal subplots). Following this, we measure the gains in terms of RSRP within an area of 125x110 meters surrounding that point. Fig. 14 showcases the impact of all the solutions (displayed in vertical subplots), including the baseline scenario, with no RIS or additional BS, for comparison (represented in the left-most column of subplots). From this example, it is evident that the RIS significantly improves RSRP in all scenarios. More notably, the largest RIS (80x80) delivers RSRP gains that are almost indistinguishable from those provided by a full-fledged BS.

To delve deeper across all the other sites, Fig. 15 presents the distribution of RSRP gains (in dB) over the baseline case, for each of the solutions mentioned above and for three different scenarios at each RIS site. The bottom and top edges of each box in the plot indicate the lower and upper quartiles of the RSRP gains, respectively, while the line in the middle represents the median RSRP gain. The whiskers depict the extreme points in the distribution.

From the figure, we can observe that even at sites with lower amounts of *harvestable* power, the RIS has a substantial impact, particularly the 80x80 RIS. For instance, the largest-scale RIS provides a median RSRP gain of 12.6 and 25.2 dB at sites C and M, respectively, and a median gain exceeding 40 dB at sites E and P. It is also evident that BS technology, comprised of energy-hungry active RF chains, offers higher RSRP gains than RIS in general. However, it is important to remember that these gains come at a significantly higher cost (we will analyze their cost-efficiency later in this section). Interestingly, in some sites, the performance of an 80x80 RIS surpasses that of a pico cell (e.g., 6.5 dB higher gains in average across sites E, F, I, and P, and more than 10x gains in sites A and H). Though micro and massive-cell antennas provide higher RSRP gains than RIS, the 80x80 RIS attains 65.1% and 61.6% of the median gains achieved by the two benchmarks, respectively, across all sites on average, and reach 84-100% of their gains in sites like H and A.

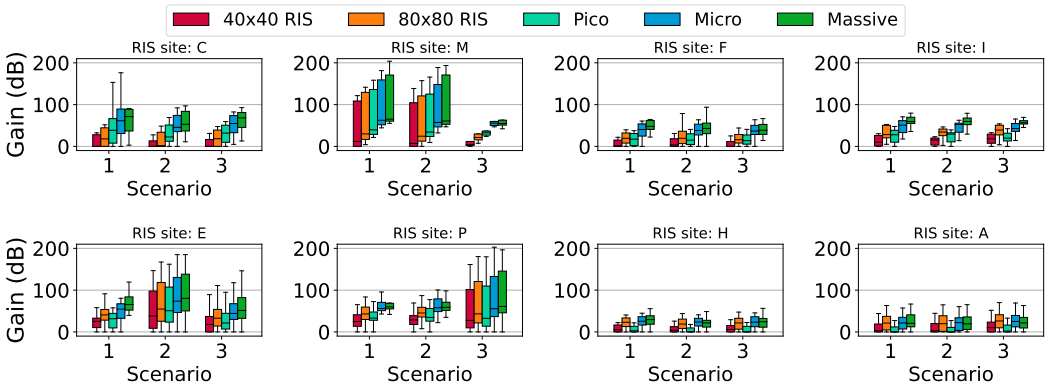

Fig. 15. Distribution of RSRP gains across eight sites with three different scenarios and solutions.

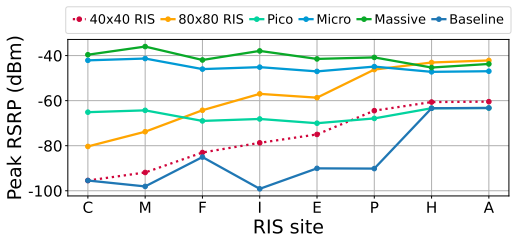

Fig. 16. Peak RSRP in the baseline case, and when using RIS and conventional BS technology.

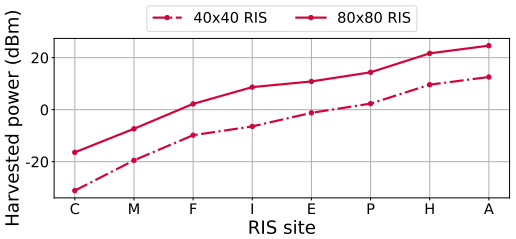

Fig. 17. Power harvested by RIS technology at each site. RIS surfaces with different sizes.

Unlike the active RF chains used by conventional radio technologies, which generate and amplify radio signals, the performance of an RIS is heavily reliant on the amount of power it can harvest from incumbent MNO cell sites. This relationship is illustrated in Fig. 16, which displays the peak RSRP experienced at each site area when different technologies are employed for coverage extension. Indeed, the performance achieved when using BS technology (pico, micro, massive-cell antennas) is practically independent of the site. In contrast, RIS technology exhibits a performance dependency that is strongly correlated with the amount of *harvestable* power, which is shown in Fig. 17. Interestingly, though the distance between the RIS site and the MNO cell sites plays a role in the amount of power a RIS can harvest, it is not the most critical aspect in highly heterogeneous urban environments – as we can note when comparing Fig. 17 and Fig. 13 – which render simple mathematical models insufficient for this type of analysis.

As previously mentioned, the RSRP gains achieved by BS technology compared to RIS technology come with associated costs. To gain insights into this, we present in Fig. 18 the ratio of RSRP gains to TCO over 5 years, a metric that we refer to as cost-gain efficiency, for each of the eight sites under consideration. To compare more cost-effective models of BS technology (remember §2.3), we also compare solutions with integrated access and backhaul (IAB). However, because micro-cells provide similar RSRP gains to massive antennas, as shown before, we only consider IAB support in the former to avoid clutter in the figure.

The figure illustrates that the large-scale 80x80 RIS significantly outperforms conventional BS technology, achieving over 3x higher efficiency on average. Even when Integrated Access and Backhaul (IAB) is supported, an 80x80 RIS still delivers 74% higher efficiency. Notably, the 40x40 RIS further amplifies these efficiency gains, doubling the efficiency of an IAB-capable micro cell on

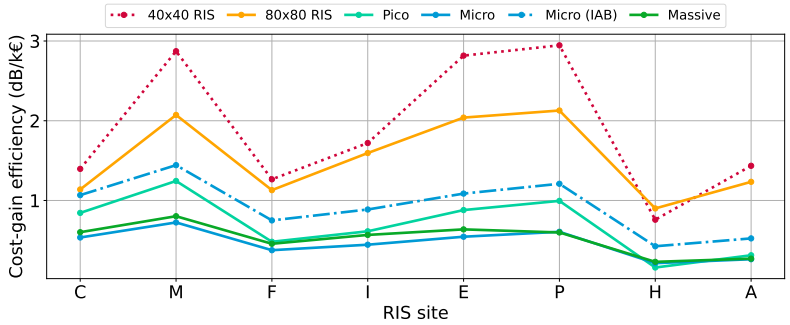

Fig. 18. Cost-gain efficiency achieved by RIS technology and conventional BS technology at different sites.

average. Perhaps surprisingly, the efficiency gap between RIS and its benchmarks has a very weak correlation with the power the RIS can harvest, or with the distance between the RIS site and the MNO cell sites. For instance, site P provides over 20 dB more power to the RIS than site F, and a RIS at site P approximately doubles the efficiency achieved at site F. Conversely, site H provides almost 30 dB higher power to the RIS than site M, but yields 56% less efficiency. These observations highlight the importance of using data-driven realistic evaluation tools when analyzing real-world scenarios. Relying on simplified models can lead to significantly erroneous results.

4.2 Coverage gains

For an MNO, ensuring broad coverage across the largest possible area is usually a high importance objective. As such, meeting specific performance targets in as many locations as possible — such as an RSRP threshold of -100 dBm in our case — typically takes precedence over achieving raw power gains. Hence, we next study the increased area where the desired coverage is achieved using all the discussed technologies (expressed as a percentage relative to the baseline coverage provided by the incumbent cell sites alone). These results are illustrated in Fig. 19.

On average, BS technology can extend coverage by around 52%, 80%, and 90% for pico, micro, and massive antennas, respectively, at sites C, M, and I. However, at site H, the increments are only 2%, 10%, and 11% respectively, while at site A, the enhancements are 10%, 25%, and 30%, respectively. Despite RIS technology not achieving these specific performance figures, it still provides considerable coverage improvements at most sites. Notably, although a 40x40 RIS yields no gains at site C, it manages to achieve between 30% and 91% of the gains of a pico-cell at various sites (M, F, E, I, P). Remarkably, it surpasses pico-cell performance by 36% and 133% at sites A and H, respectively, due to its superior beamforming capabilities. Conversely, an 80x80 RIS outperforms a pico-cell antenna at all sites except C and M, tripling or even quadrupling the coverage area at certain sites such as A and H, respectively. When compared to a micro or a massive-cell antenna, an 80x80 RIS reaches 72% and 68% of the coverage area gains of these benchmarks, respectively, on average across all sites.

As remarked before, RIS technology can boost performance while significantly curbing costs. We verify this by determining the ratio of area coverage gains (expressed as a percentage) to their associated costs — a measure we refer to as cost-coverage efficiency. These findings are depicted in Fig. 20 for each site considered in this study.

Except for site C, RIS technology provides higher cost-coverage efficiency than its benchmarks across all sites. At site C, the 40x40 RIS fails to enhance coverage, thereby delivering 0% cost-coverage efficiency, while the 80x80 RIS, despite offering 29% greater cost-efficiency than a standard micro-cell, reaches 65% of the cost-efficiency of an IAB-capable micro-cell antenna. The main reasons why Site C performs so poorly, especially for the 40x40 RIS case, are attributed to low

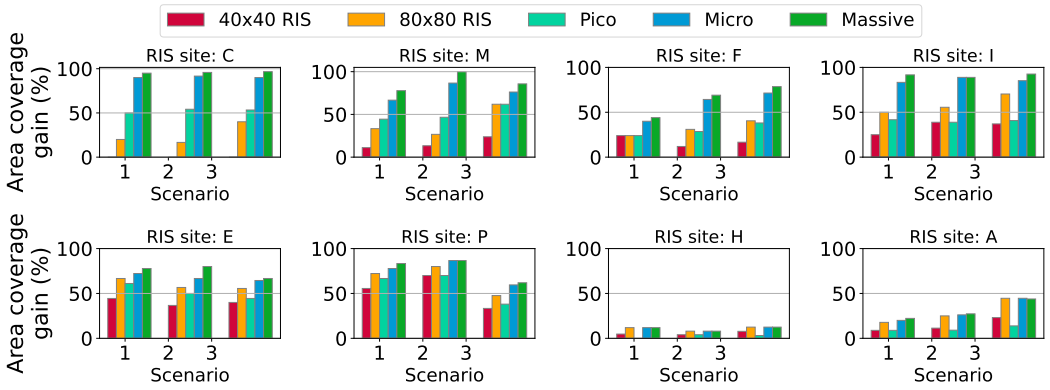

Fig. 19. Area coverage gains across eight sites with three different scenarios and solutions.

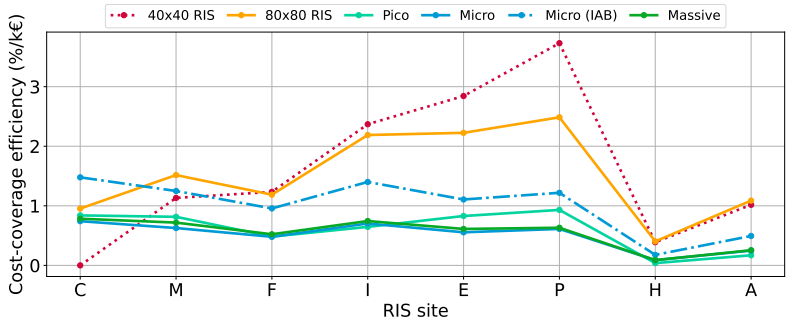

Fig. 20. Cost-coverage efficiency achieved by RIS and conventional BS technology at different sites.

elevation and suboptimal building orientation towards the base station; this underscores how crucial correct positioning is for an RIS to function at its best. Remarkable gains are recorded at other sites. For example, the 80x80 RIS doubles the cost-efficiency of both micro and massive active antennas at sites M and F, triples it at site I, and quadruples it at sites E, P, H, and A. Compared with an IAB-supported micro-cell antenna, the 80x80 RIS doubles the performance at sites E, P, H, and A, and delivers between 20% and 50% increased cost-efficiency at sites M, F, and I. Interestingly, at certain sites, such as I, E, and P, a 40x40 RIS surpasses its larger 80x80 counterpart. Across all sites, RIS technology presents cost-efficiency gains that vary from approximately 50% more than an IAB-supported micro-cell antenna to four times the cost-efficiency of a conventional micro-cell or massive active antenna.

In conclusion, our findings strongly advocate for RIS as a cost-effective solution for expanding coverage in real-world urban mobile networks. Even with non-ideal RIS models, such as the data-driven approach we explored in this paper, RIS technology typically outperforms the cost-effectiveness of alternatives with active antennas. This is achieved through two key factors: (*i*) the use of affordable electronic components with minimal energy consumption, and (*ii*) the vast array of beamforming-capable antenna elements provided by RIS technology, which enable radio and coverage enhancements that closely compete with those of conventional BS technologies relying upon active RF chains. However, our results also highlight that while RIS technology generally offers higher efficiency in terms of RSRP gains per unit cost at all analyzed sites, these may be insufficient to meet coverage targets. Indeed, we found that certain RIS scales (e.g., 40x40 RIS) may not yield any coverage enhancements at some sites (6% of the sites in our study), or may offer lower cost-coverage efficiency than BS technology at others (10% in our study). This underscores the

need for appropriate data-driven methods, like those employed in this paper, to accurately select coverage-enhancing sites and the most suitable technology to this end.

5 TOWARDS REAL-WORLD DEPLOYMENTS

While RIS technology is continuously evolving to address current challenges, it brings to operators' attention its immense potential, especially in terms of considerably reducing their energy footprint when deploying the next generation of communication systems. Multiple telco operators have recently shown interest in testing this technology, either with radio network planning exercises (using ray-tracing approaches) or in field trials (using prototypes in a test network) [2, 25].

When evaluating 5G communication technologies, standard development organizations (SDOs) such as 3GPP [40] and ETSI [12] usually rely on a map-based hybrid channel modeling approach. In general, ray-tracing methods — such as the one we used in this paper — are useful for mobile operators to plan large-scale deployments. It is therefore not surprising that radio planning teams in telcos worldwide use them. For instance, Atoll is a tool currently being used by operators in several large telcos in Europe, including Orange, Vodafone, and Telefonica [8], and operators such as Huawei [19] and Telefonica [1] routinely use these tools in network planning.

In our paper, we took a step further when using ray-tracing to analyze the potential of RIS technology on large-scale deployments. Instead of using ideal reflector models, we captured the imperfections of realistic RIS equipment and integrated this model into the ray-tracing framework, as explained in §2.2. We believe that this approach provides compelling evidence of the potential of RIS technology in real environments as RIS hardware is purposely intended to be low-cost technology, which is prone to imperfections. We will further improve this approach by considering higher density and more accurate empirical radio coverage measurements to calibrate the ray-tracing modules we employ. This will help us generate an even more accurate evaluation of the benefit of deploying RIS in operational networks.

In light of the results we presented in this paper, our next step is to validate some of our insights with already-planned field trials with Telefonica and Telecom Italia in 2024. We will conduct these in testing and controlled environments, which represents the natural next step before deployment in large-scale production RANs. These trials will help us answer multiple practical questions about the manufacturing and installation of these devices, which is not trivial. When considering RIS installation in a commercial network, finding the optimal location is important; in practical terms, the deployment is also conditioned by negotiating new deployment sites for the telcos. The planned pilots will help us gauge the distance between the optimal identified installation locations and the locations we can use under the constraints of the real-world environment.

6 RELATED WORKS

The existing body of literature on RIS has provided valuable insights into this promising technology. For instance, the importance of RIS placement has been thoroughly discussed in [16], [18], and [15], which have theoretically explored the ideal distance between the BS and RIS.

The authors of [4] have made a significant contribution by addressing the challenges of determining the optimal RIS placement and configuration without making unrealistic assumptions about the available Channel State Information. However, their work is confined to indoor scenarios, limiting its applicability in broader contexts, and assuming idealized RIS models. In contrast, our study extends this analysis to real-world, large-scale outdoor RIS-aided mobile networks, providing a more comprehensive understanding of RIS technology's potential. The research conducted by [26] introduces a novel mathematical formulation for the coverage planning problem. While their theoretical approach provides a solid foundation, our work complements this by providing empirical

evidence from a production mobile network, offering a more practical perspective on the deployment of RIS technology. In [29], the authors delve into the complexity requirements of large RIS deployments, providing valuable insights into the optimal configuration of these systems. However, their work is based on simulations, whereas our study is grounded in real-world data, offering a more accurate assessment of RIS technology's effectiveness. Finally, [35] employs the QuaDRiGa channel model to optimize the positioning and orientation of a RIS. While their methodology is practical, it lacks the empirical validation provided by our study.

The existing literature is somewhat sparse when it comes to cost-efficiency analyses. Notable work is presented in [22], where the authors explore the costs associated with deploying RIS and ultra-dense small-cells for indoor mmWave coverage enhancement. Their findings suggest that RIS may offer cost savings, but only with sufficient small-cell densification. However, their analysis is grounded in simple propagation models and primarily applies to smaller systems.

In conclusion, while the existing literature has made significant strides in understanding RIS technology, our paper is, to the best of our knowledge, the first to analyze the cost-effectiveness of real-world large-scale RIS technology in production mobile networks. This unique focus allows us to provide valuable insights into the practical application of RIS technology, contributing to the ongoing development of next-generation mobile systems.

7 CONCLUSION

RIS technology is a promising solution for next-generation mobile systems, especially in a vying landscape where operators are striving to dramatically reduce their energy footprint and optimize the cost of running their infrastructure. To the best of our knowledge, this paper is the first to bring compelling evidence towards harvesting the huge potential of RIS technology in the realistic outdoor deployments of a commercial mobile operator. In this paper, we showed that, in real-world urban mobile networks, RIS can achieve 72% of the coverage extension gains of conventional base station technologies based on active antennas, but at only 22% of the total cost of ownership over a five-year period, offering around three times higher cost-efficiency.

To quantify the benefits upon deployment in a production radio network, we aligned our approach with the methodology that operational radio planning teams follow: we combined different empirical datasets provided by a commercial radio network in the UK to evaluate coverage, we used a realistic data-driven RIS model, and we employed a state-of-the-art ray tracing tool that we validated with real data to answer complex "what-if" questions regarding the deployment of the RIS in real-world outdoor scenarios. To the best of our knowledge, our results provide the first estimation of the benefits we can expect from RIS when exploited in a commercial radio network deployment. As future work, we are planning live outdoor trials to experimentally evaluate RIS prototypes in the network of commercial operators.

ACKNOWLEDGMENTS

The research leading to these results has received funding from the EU FP for Research and Innovation Horizon 2020 under Grant Agreements No. 861222 (MINTS), No. 101017109 (DAEMON project), No. 101017011 (RISE-6G). The work has also been supported by the Spanish Ministry of Economic Affairs and Digital Transformation and the European Union – NextGeneration EU, in the framework of the Recovery Plan, Transformation and Resilience (PRTR) (Call UNICO I+D 5G 2021, ref. number TSI-063000-2021-59, and the UNICO I+D 5G SORUS project).

REFERENCES

[1] [n. d.]. Private communications with Maria Teresa Aparicio Peña. Head of Open RAN, Telefónica.

[2] 2023. *World's First Dynamic RIS Trial Boosts mmWave Network Performance.* https://www.telecomreviewasia.com/news/network-news/3567-world-s-first-dynamic-ris-trial-boosts-mmwave-network-performance Accessed on 2023-10-09.

[3] 75Media. n.d.. *Billboard Costs.* https://75media.co.uk/blog/billboard-costs/ Accessed in April 2023.

[4] Antonio Albanese, Guillermo Encinas-Lago, Vincenzo Sciancalepore, Xavier Costa-Pérez, Dinh-Thuy Phan-Huy, and Stéphane Ros. 2022. RIS-aware indoor network planning: The Rennes railway station case. In *ICC 2022-IEEE International Conference on Communications*. IEEE, 2028–2034.

[5] Ufuk Altun and Ertugrul Basar. 2021. Ris enabled secure communication with covert constraint. In *2021 55th Asilomar Conference on Signals, Systems, and Computers*. IEEE, 685–689.

[6] Imran Ashraf, Federico Boccardi, and Lester Ho. 2011. Sleep mode techniques for small cell deployments. *IEEE Communications Magazine* 49, 8 (2011), 72–79.

[7] Atoll. 2023. Atoll Overview. https://www.forsk.com/atoll-overview Accessed on June 12, 2023.

[8] Atoll. n.d.. *Atoll at Three in Europe.* https://www.forsk.com/news/atoll-three-europe Accessed in September 2023.

[9] Xiaoyuan Cheng, Yukun Hu, and Liz Varga. 2022. 5G network deployment and the associated energy consumption in the UK: A complex systems' exploration. *Technological Forecasting and Social Change* 180 (2022), 121672.

[10] Marco Di Renzo, Alessio Zappone, Merouane Debbah, Mohamed-Slim Alouini, Chau Yuen, Julien De Rosny, and Sergei Tretyakov. 2020. Smart radio environments empowered by reconfigurable intelligent surfaces: How it works, state of research, and the road ahead. *IEEE journal on selected areas in communications* 38, 11 (2020), 2450–2525.

[11] Manideep Dunna, Chi Zhang, Daniel Sievenpiper, and Dinesh Bharadia. 2020. ScatterMIMO: Enabling virtual MIMO with smart surfaces. In *Proceedings of the 26th Annual International Conference on Mobile Computing and Networking*. 1–14.

[12] ETSI. 2023. ETSI TS 103 324: Intelligent Transport System (ITS); Vehicular Communications; Basic Set of Applications; Collective Perception Service; Release 2. Technical Specification.

[13] Eurostat. [n. d.]. Electricity price statistics. Accessed in April 2023. URL: https://ec.europa.eu/eurostat/statistics-explained/index.php?title=Electricity_price_statistics#Electricity_prices_for_non-household_consumers.

[14] Ziheng Fu, Swagato Mukherjee, Michael T Lanagan, Prasenjit Mitra, Tarun Chawla, and Ram M Narayanan. 2022. Optimization of 5G Infrastructure Deployment Through Machine Learning. In *2022 IEEE International Symposium on Antennas and Propagation and USNC-URSI Radio Science Meeting (AP-S/URSI)*. IEEE, 1684–1685.

[15] Gourab Ghatak. 2021. On the placement of intelligent surfaces for RSSI-based ranging in mm-wave networks. *IEEE Communications Letters* 25, 6 (2021), 2043–2047.

[16] Hiroaki Hashida, Yuichi Kawamoto, and Nei Kato. 2020. Intelligent reflecting surface placement optimization in air-ground communication networks toward 6G. *IEEE Wireless Communications* 27, 6 (2020), 146–151.

[17] Rizqi Hersyandika, Marco Rossanese, Andra Lutu, Yang Miao, Qing Wang, and Sofie Pollin. 2023. Coverage and Capacity Analysis for Football Player's Bodycam with Cell-Free Massive MIMO. *IEEE* (2023).

[18] Pei-Qiu Huang, Yu Zhou, Kezhi Wang, and Bing-Chuan Wang. 2022. Placement optimization for multi-IRS-aided wireless communications: An adaptive differential evolution algorithm. *IEEE Wireless Communications Letters* 11, 5 (2022), 942–946.

[19] Huawei. 2018. Huawei 5G Wireless Network Planning Solution White Paper. *White Paper* (2018).

[20] Infovista. 2023. 5G Network Planning, Testing and Assurance Automation. https://www.infovista.com/ Accessed on June 12, 2023.

[21] Klas Johansson, Anders Furuskar, Peter Karlsson, and Jens Zander. 2004. Relation between base station characteristics and cost structure in cellular systems. In *2004 IEEE 15th International Symposium on Personal, Indoor and Mobile Radio Communications (IEEE Cat. No. 04TH8754)*, Vol. 4. IEEE, 2627–2631.

[22] Zeyang Li, Haonan Hu, Jiliang Zhang, and Jie Zhang. 2021. Enhancing Indoor mmWave Wireless Coverage: Small-Cell Densification or Reconfigurable Intelligent Surfaces Deployment? *IEEE Wireless Communications Letters* 10, 11 (2021), 2547–2551. https://doi.org/10.1109/LWC.2021.3106821

[23] Christos Liaskos, Shuai Nie, Ageliki Tsioliaridou, Andreas Pitsillides, Sotiris Ioannidis, and Ian Akyildiz. 2018. A new wireless communication paradigm through software-controlled metasurfaces. *IEEE Communications Magazine* 56, 9 (2018), 162–169.

[24] Alfio Lombardo. 2019. Cost Analysis of Orchestrated 5G Networks for Broadcasting. *EBU Tech Review* (2019). https://tech.ebu.ch/docs/techreview/EBU_Tech_Review_2019_Lombardo_Cost_analysis_of_orchestrated_5G_networks_for_broadcasting.pdf

[25] Christian Mokry. 2023. *Rohde & Schwarz and Greenerwave Collaborate to Verify RIS Modules and Drive 6G Research.* https://www.rohde-schwarz.com/es/acerca-de/noticias-y-prensa/all-news/rohde-schwarz-and-greenerwave-collaborate-to-verify-ris-modules-and-drive-6g-research-comunicados-de-prensa-pagina-de-detalles_229356-1404099.html Accessed on 2023-10-09.

[26] Eugenio Moro, Ilario Filippini, Antonio Capone, and Danilo De Donno. 2021. Planning Mm-Wave access networks with reconfigurable intelligent surfaces. In *2021 IEEE 32nd Annual International Symposium on Personal, Indoor and Mobile Radio Communications (PIMRC)*. IEEE, 1401–1407.

[27] Edward J Oughton, Zoraida Frias, Sietse van der Gaast, and Rudolf van der Berg. 2019. Assessing the capacity, coverage and cost of 5G infrastructure strategies: Analysis of the Netherlands. *Telematics and Informatics* 37 (2019), 50–69.

[28] Xilong Pei, Haifan Yin, Li Tan, Lin Cao, Zhanpeng Li, Kai Wang, Kun Zhang, and Emil Björnson. 2021. RIS-aided wireless communications: Prototyping, adaptive beamforming, and indoor/outdoor field trials. *IEEE Transactions on Communications* 69, 12 (2021), 8627–8640.

[29] Andreia Pereira, Fredrik Rusek, Marco Gomes, and Rui Dinis. 2022. Deployment Strategies for Large Intelligent Surfaces. *IEEE Access* 10 (2022), 61753–61768.

[30] Junhui Rao, Yujie Zhang, Shiwen Tang, Zan Li, Chi-Yuk Chiu, and Ross Murch. 2023. An Active Reconfigurable Intelligent Surface Utilizing Phase-Reconfigurable Reflection Amplifiers. *IEEE Transactions on Microwave Theory and Techniques* (2023).

[31] Remcom. 2023. Wireless InSite - 3D Wireless Prediction Software. https://www.remcom.com/wireless-insite-em-propagation-software

[32] Marco Rossanese, Placido Mursia, Andres Garcia-Saavedra, Vincenzo Sciancalepore, Arash Asadi, and Xavier Costa-Perez. 2022. Designing, building, and characterizing RF switch-based reconfigurable intelligent surfaces. In *Proceedings of the 16th ACM Workshop on Wireless Network Testbeds, Experimental evaluation & CHaracterization*. 69–76.

[33] Juan Rendon Schneir, Ade Ajibulu, Konstantinos Konstantinou, Julie Bradford, Gerd Zimmermann, Heinz Droste, and Rafael Canto. 2019. A business case for 5G mobile broadband in a dense urban area. *Telecommunications Policy* 43, 7 (2019), 101813.

[34] Wankai Tang, Ming Zheng Chen, Xiangyu Chen, Jun Yan Dai, Yu Han, Marco Di Renzo, Yong Zeng, Shi Jin, Qiang Cheng, and Tie Jun Cui. 2020. Wireless communications with reconfigurable intelligent surface: Path loss modeling and experimental measurement. *IEEE Transactions on Wireless Communications* 20, 1 (2020), 421–439.

[35] Ehsan Tohidi, Sven Haesloop, Lars Thiele, and Slawomir Stanczak. 2023. Near-Optimal LOS and Orientation Aware Intelligent Reflecting Surface Placement. *arXiv preprint arXiv:2305.03451* (2023).

[36] Igor A Tomić, Milutin S Davidović, and Sanja M Bjeković. 2015. On the downlink capacity of LTE cell. In *2015 23rd Telecommunications Forum Telfor (TELFOR)*. IEEE, 181–185.

[37] Georgios C Trichopoulos, Panagiotis Theofanopoulos, Bharath Kashyap, Aditya Shekhawat, Anuj Modi, Tawfik Osman, Sanjay Kumar, Anand Sengar, Arkajyoti Chang, and Ahmed Alkhateeb. 2022. Design and evaluation of reconfigurable intelligent surfaces in real-world environment. *IEEE Open Journal of the Communications Society* 3 (2022), 462–474.

[38] Yu Zhang and Ahmed Alkhateeb. 2023. Deep Learning of Near Field Beam Focusing in Terahertz Wideband Massive MIMO Systems. *IEEE Wireless Communications Letters* 12, 3 (2023), 535–539. https://doi.org/10.1109/LWC.2022.3233566

[39] Zijian Zhang, Linglong Dai, Xibi Chen, Changhao Liu, Fan Yang, Robert Schober, and H Vincent Poor. 2022. Active RIS vs. passive RIS: Which will prevail in 6G? *IEEE Transactions on Communications* 71, 3 (2022), 1707–1725.

[40] Qiuming Zhu, Cheng-Xiang Wang, Boyu Hua, Kai Mao, Shan Jiang, and Mengtian Yao. 2021. *3GPP TR 38.901 Channel Model*. John Wiley Sons, Ltd, 1–35. https://doi.org/10.1002/9781119471509.w5GRef048 arXiv:https://onlinelibrary.wiley.com/doi/pdf/10.1002/9781119471509.w5GRef048

Received July 2023; accepted October 2023